Peak velocities estimation for a direct five-step design procedure of inter-storey viscous dampers

Peak velocities estimation for a direct five-step design procedure of inter-storey viscous dampers

Michele Palermo [1], Stefano Silvestri, Luca Landi, Giada Gasparini and Tomaso Trombetti

Department DICAM, University of Bologna, Viale Risorgimento 2, 40136 Bologna, Italy

ABSTRACT

In the last decades, the use of added viscous dampers for the mitigation of the effects due to the seismic action upon the structural elements has been worldwide spread. In this respect, several design methods aimed at sizing the viscous dampers to be inserted in building structures have been proposed. Among others, some of the authors proposed a five-step procedure which guides the practical design from the choice of a target reduction in the seismic response of the structural system (with respect to the response of a structure without any additional damping devices), to the identification of the corresponding damping ratio and the mechanical characteristics (i.e. the damping coefficient values for chosen damping exponent, the oil stiffness) of the commercially available viscous dampers. The procedure requires the development of numerical simulations for the evaluations of the peak inter-storey velocity profiles, necessary for the evaluation of the damper forces. In the present paper a comprehensive study on the inter-storey velocity profiles developed in shear-type building structures under seismic excitations is conducted with the purpose of deriving analytical formulae for their estimation. The analytical estimations of the peak inter-storey velocities are then used to simplify the original five-step procedure leading to a direct (i.e. fully analytical) procedure. The direct procedure is suitable for the preliminary design of the added viscous dampers, in particular for practitioners not dealing everyday with the design of added viscous dampers.

---

[1] Corresponding author. Phone: +39 051 20 9 3232; Fax: +39 051 20 9 3236; e-mail: michele.palermo7@unibo.it

1. INTRODUCTION

Manufactured viscous dampers are hydraulic devices which can be inserted in building structures in order to mitigate the seismic effects through the dissipation of part of the kinetic energy by an earthquake to the structure (Soong and Dargush 1997, Constantinou et al. 1998, Hart and Wong 2000, Chopra 1995, Christopoulos and Filiatrault 2006). The effectiveness of such devices in reducing the seismic demand on the structural elements has been demonstrated by a number of research works since the 1980s (Constantinou and Tadjbakhsh 1983, Constantinou and Symans 1992 and 1993, Trombetti and Silvestri 2004, 2006 and 2007, Silvestri and Trombetti 2007, Takewaki 2009, Occhiuzzi 2009, Silvestri et al. 2011, Diotallevi et al. 2012, Palermo et al. 2013b, Hwang et al. 2013, Landi et al. 2013 and 2014). Most of the research works on viscous dampers (Takewaki 1997, 2000 and 2009, Shukla and Datta 1999, Lopez Garcia 2001, Singh and Moreschi 2002, Levy and Lavan 2006) basically propose sophisticated numerical algorithms for dampers optimization, i.e. damper size and location, sometimes leading to complex design procedures. Nevertheless, the application of such algorithms often requires computational expertise and time (beyond the typical availabilities of the designers) and relies mainly upon numerical results which do not provide physical insight into the matter.

As far as the seismic design of "traditional structures" (i.e. not equipped with additional viscous dampers) is concerned, it is to be noted that, even though the most recent tools for the seismic analysis of building structures are based upon sophisticated time-history simulations, the milestones and the fundamental developments of earthquake engineering have been always based on simple tools (e.g. the response spectrum concept) which allow engineers to understand and control the structural behaviour under seismic excitation. A typical example is the equivalent static force method (lateral force method, according to Eurocode 8) based upon the first mode contribution, which, even though is nowadays surpassed by more sophisticated procedures, still retains its validity.

On the other hand, as far as the seismic design of structures equipped with additionally viscous dampers is concerned, the issue of developing simple/analytical methods in order to size and locate the viscous dampers is still open.

In 1992, report NCEER-92-0032 (Constantinou and Symans 1992) first investigated the problem of selecting the damping coefficients of linear viscous dampers in an elastic system to provide a specific damping ratio. In 2000, report MCEER-00-0010 (Ramirez et al. 2000) proposed an analytical relationship between the viscous damping ratio in a given mode of vibration and the damping coefficients using energy-based criteria (Uang and Bertero 1990, Filiatrault et al. 1994, Costantinou et al. 1998), assuming a given undamped mode shape. ASCE 7 (2005) Chapter 18, which is grounded on the MCEER-00-0010 approach and on the works by Ramirez et al. (2002a and b, and 2003) and by Whittaker et al. (2003), contains systematic linear and non-linear procedures for design and analysis of building with damping systems, including prediction of damper velocities and damper forces accounting also for the higher mode effects (on drift, velocity, acceleration and forces) by making use of the residual mode approach. The methodology of Ramirez and co-workers that form the ASCE 7 (2005) Chapter 18 procedures can be applied to all types of damping systems and has been successfully validated also with reference to yielding structures Ramirez et al. (2003).

Alternative approaches leading to practical design procedures for the sizing of viscous dampers have been proposed in the last years: (i) Lopez-Garcia 2001 developed a simple algorithm for optimal damper configuration (placement and properties) in MDOF structures, assuming a constant inter-storey height and a straight-line first modal shape; (ii) Christopoulos and Filiatrault (2006) suggested a design approach for estimating the damping coefficients of added viscous dampers consisting in a trial and error procedure; (iii) Silvestri et al. (2010) proposed a direct design approach, referred to as the "five-step procedure".

This latter five-step procedure aims at guiding the professional engineer from the choice of the target objective performance (reduction of significant response quantities with respect to a 5% damped system) to the identification of the mechanical characteristics (i.e. damping coefficient, oil stiffness, maximum damper forces) of commercially available viscous dampers. The original procedure (Silvestri et al. 2010, Silvestri et al. 2011, Palermo et al. 2013a) although mostly based on analytical expressions, still requires the development of numerical time-history analyses of FE models in order to estimate the maximum inter-storey velocity, necessary to obtain the maximum forces in the added

dampers. This step inhibits the completion of the damper sizing relying on analytical results only, useful for preliminary design and for subsequent check of numerical results. The identification of an analytical expression of the inter-storey velocity profiles would allow the designer to directly obtain the maximum dampers forces (often a key parameter for the evaluation of the dampers cost), without performing numerical simulations. In this regard, in 1999, Peckan examined the difference between actual relative velocity and pseudo-velocity in SDOF systems subjected to earthquake excitation. The study by Miranda and Akkar 2006 highlighted the significant discrepancies between first mode drifts and total drifts in MDOF structures by introducing the concept of generalized inter-storey drift spectrum. A recent work by Adachi et al. (2013) acknowledged that the distribution of the maximum inter-storey velocities is a key index in order to evaluate the along-height demand on viscous dampers and exhibit specific characteristics depending on the number of the storeys of the building.

The above mentioned studies clearly showed that the pseudovelocity may significantly differs from the actual relative velocity and that, for long period structures, the higher modes lead to a significant increase of the inter-storey drifts and velocities.

In the present paper, first, a study on the peak inter-storey velocity profiles of frame building structures equipped with inter-storey dampers and subjected to earthquake excitation has been conducted, and analytical estimates of the peak inter-storey velocities have been derived (the "average" contribution of the higher modes is taken into account by introducing a correction factor as a linear function of the fundamental period). Second, the obtained estimates have been used to simplify the five-step procedure, leading to a direct and practical procedure, which allows to condense the preliminary sizing of the viscous dampers in a single direct formula.

2. AN ESTIMATION OF THE PEAK FIRST MODE INTER-STOREY VELOCITIES

It is of common belief that the effectiveness of dampers allocation is closely related to the inter-storey drift demand. However, a recent work (Adachi et al. 2013) showed that, while this understanding is approximately true in rather low-

to medium-rise buildings, the key parameter for the estimation of the damping forces in high-rise buildings equipped with inter-storey dampers turns out to be the along-the-height distribution of the maximum inter-storey velocities. This distribution may substantially differ (in terms of shape) with respect to that of the maximum inter-storey drifts due to a more significant higher modes contribution. In the same work, the authors also introduced approximate predictions for the maximum horizontal force of linear viscous dampers. In detail, correction factors are introduced to account for the contribution of the higher modes.

In this section, a study on the inter-storey velocity profiles is carried out with the purpose of obtaining an analytical estimation of the maximum inter-storey velocity starting from an assumed displacement profile along the height of the building.

Let us consider a *N*-storey shear-type building structure with uniform floor mass distribution. Two estimations based on two different first-mode deformed shapes (drift profiles) are hereafter presented.

2.1. Profile A

Let's assume that the first mode peak displacement profile under seismic excitation is equal to:

$$\left\{\phi^1\right\}_A = \beta \left\{ \begin{array}{c} \dfrac{N(N+1)}{2} \\ ... \\ i\,\dfrac{N(N+1)}{2} - \displaystyle\sum_{j=0}^{i-1}\dfrac{j(j+1)}{2} \\ ... \\ \dfrac{N^2(N+1)}{2} - \displaystyle\sum_{j=0}^{N-1}\dfrac{j(j+1)}{2} \end{array} \right\} \tag{1}$$

where *i* represents the *i*-th storey and β is a constant depending on the seismic intensity and on the first modal contribution factor (Chopra 1995). *N* indicates the total number of storeys. The modal shape of Eq. (1) may be interpreted as the first approximation of the exact first eigenvector as obtained using the Rayleigh-Ritz method (starting from a linear distribution of static forces along the building height) of a uniform (i.e. constant lateral stiffness at all floors) shear-type system. The pseudo-velocity and pseudo-acceleration profiles are here defined as follows:

$$\left\{\dot{\phi}^1\right\}_A = \omega_1 \left\{\phi^1\right\}_A \tag{2}$$

5

$$\left\{ \ddot{\phi}^{1} \right\}_{A} = \omega_{1}^{2} \left\{ \phi^{1} \right\}_{A} \tag{3}$$

From structural dynamics (Chopra 1995), the base shear, V_{base}, can be evaluated as follows:

$$V_{base} = m_{tot} \cdot S_{a} \tag{4}$$

where $m_{tot} = N \cdot m$ is the total building mass, and S_a is the pseudo-acceleration at the centre of gravity of the building.

By assuming that the base shear is given entirely by the first mode (conservative assumption which can be considered reasonable for the case of regular frame structures (Chopra 1995)):

$$V_{base} = \left\{ m \right\}^{T} \cdot \left\{ \ddot{\phi}^{1} \right\}_{A} \tag{5}$$

where $\{ m \}$ is the vector of the floor masses (lumped masses are assumed).

The constant β is then obtained by equating Eqs. (4) and (5):

$$N \cdot m \cdot S_{a} = \sum_{i=1}^{N} m \cdot \beta \cdot \omega_{1}^{2} \left[i \frac{N(N+1)}{2} - \sum_{j=0}^{i-1} \frac{j(j+1)}{2} \right] \tag{6}$$

leading to:

$$\beta = \frac{S_{a}}{\omega_{1}^{2}} \frac{24}{(N+1)(2+5N+5N^{2})} \tag{7}$$

By substituting Eq. (7) into Eq. (1) and Eq. (2), after some mathematical developments, the following analytical expressions of the peak inter-storey drift and peak inter-storey pseudo-velocity profiles under seismic input are obtained:

$$\left\{ \delta^{1} \right\}_{A} = \frac{S_{a}}{\omega_{1}^{2}} \frac{24}{(N+1)(2+5N+5N^{2})} \left\{ \begin{array}{c} \frac{N(N+1)}{2} \\ \dots \\ \frac{N(N+1)}{2} - \frac{i(i-1)}{2} \\ \dots \\ \frac{N(N+1)}{2} - \frac{N(N-1)}{2} \end{array} \right\} \tag{8}$$

$$\left\{ \dot{\delta}^{1} \right\}_{A} = \frac{S_{a}}{\omega_{1}} \frac{24}{(N+1)(2+5N+5N^{2})} \left\{ \begin{array}{c} \frac{N(N+1)}{2} \\ \dots \\ \frac{N(N+1)}{2} - \frac{i(i-1)}{2} \\ \dots \\ \frac{N(N+1)}{2} - \frac{N(N-1)}{2} \end{array} \right\} \tag{9}$$

6

It can be noted that the largest value of $\{\dot{\delta}^1\}_A$, $v_{max,A}$, is achieved at the first inter-storey, $\dot{\delta}_1^1$:

$$v_{max,A} = \dot{\delta}_1^1 = \frac{S_a}{\omega_1} \cdot \frac{12N}{(2 + 5N + 5N^2)} \tag{10}$$

This analytical formula may be used for buildings with nearly uniform floor mass and lateral storey stiffness distributions and stiff beams, which may ensure a shear-type behavior.

2.2. Profile B

Let's assume a linear first mode peak displacement profile:

$$\{\phi^1\}_B = \beta \begin{Bmatrix} 1 \\ \dots \\ i \\ \dots \\ N \end{Bmatrix} \tag{11}$$

In this case, by means of the same mathematical developments detailed above, the peak inter-storey pseudo-velocity under seismic input is equal at all storeys and is given by:

$$v_{max,B} = \frac{S_a}{\omega_1} \cdot \frac{2}{N+1} \tag{12}$$

This analytical formula is appropriate for a moment resisting frame characterized by a nearly linear first mode shape. As illustrative example, the study of Akkar et al. (2005), which analysed the drift profiles for different beam-to-column stiffness ratios, showed that the first mode shapes of 3-, 9-, and 20-storey Los Angeles Pre-Northridge Design SAC steel frames are nearly linear (see Figs. 2 a–c of Akkar et al. 2005).

In general, once a FE model of the building is developed, the choice of the more appropriate drift profile (Eq. 1 and 11) can be verified by means of the modal analysis and, in particular, by comparing the actual first mode shape with the two proposed profiles displayed in Fig. 1A.

3. PEAK INTER-STOREY VELOCITIES FROM NUMERICAL TIME-HISTORY SIMULATIONS

With the purpose of verifying the effectiveness of the predictive formulations of the peak inter-storey velocities for shear-type frame structures given by Eqs. 9 and 10 and of identifying their limits of validity, an extensive parametric study has been conducted. For sake of conciseness, this section presents only the relevant results obtained from this study.

3.1. The studied systems

Two types of shear-type (ST) systems are investigated:

- Type A: shear-type structures with uniform (along the height) mass and stiffness distribution;

- Type B: shear-type structures with uniform (along the height) mass distribution and storey stiffness k_i (i indicating the i-th storey) leading to an exact linear first-mode deformed shape:

$$k_i = \lambda \frac{N(N+1) - i(i-1)}{2} \tag{13}$$

where λ is a generic constant given that Eq. (13) indicates a profile.

For the sake of clearness, the first mode drift and inter-storey drift profiles (normalized) of a 10-storey Type A and Type B structures are represented in Figure 1.

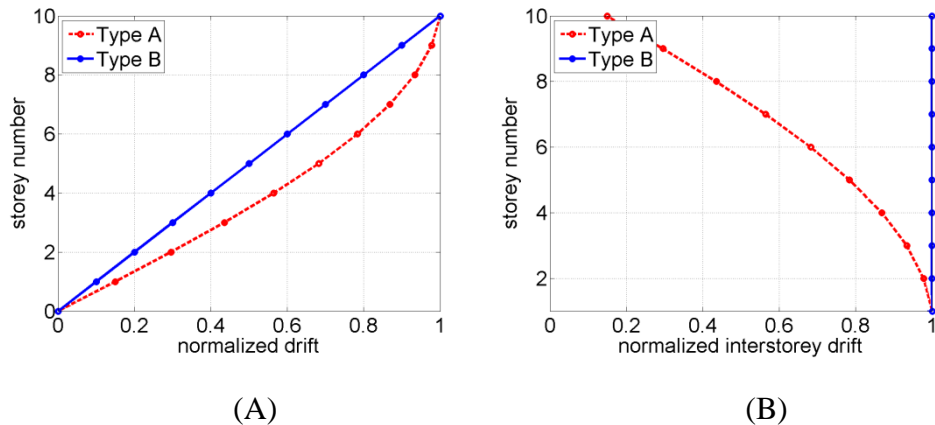(A)   (B)

Figure 1 First mode drift (A) and inter-storey drift (B) profiles for Type A and Type B structures (10-storey building).

The properties of the shear-type systems here considered are:

- total number of storeys N selected between 5 and 30;

- uniform floor mass $m = 100$ ton;

- storey stiffness $\rho_k k_i$ (with k_i given in Table 1, and ρ_k equal to 0.5, 1.0, 2.0 and 5.0) in order to cover a range of fundamental periods between 0.1 s to 5.0 s (i.e. covering the range of low- to high-rise frame structures);

- total damping coefficient c_{tot} (according to the original five-step procedure by Silvestri et al. (2010)) leading to damping ratios $\xi = 0.05$, 0.15, 0.30;

- two distributions of dampers along the height of the building are considered: uniform (U) and stiffness proportional (SP).

Table 1: k_i values for the considered structures.

	storey	$N = 5$	$N = 10$	$N = 20$	$N = 30$
Type A constant k at all storeys [kN/m]		1000000	1000000	1000000	1000000
Type B k_i [kN/m]	1	2608203	2790622	2891556	2926826
	2	2332847	2647417	2818340	2877632
	3	2020305	2496008	2743171	2827583
	4	1649572	2334802	2665883	2776631
	5	1166424	2161607	2586286	2724727
	6	/	1973268	2504161	2671814
	7	/	1764944	2419249	2617833
	8	/	1528487	2331247	2562714
	9	/	1248004	2239789	2506384
	10	/	882472	2144435	2448758
	11	/	/	2044639	2389743
	12	/	/	1939715	2329234
	13	/	/	1828780	2267110
	14	/	/	1710667	2203235
	15	/	/	1583770	2137452
	16	/	/	1445778	2069579
	17	/	/	1293143	1999403
	18	/	/	1119895	1926673
	19	/	/	914390	1851087
	20	/	/	646572	1772281
	21	/	/	/	1689804
	22	/	/	/	1603089
	23	/	/	/	1511406
	24	/	/	/	1413791
	25	/	/	/	1308916
	26	/	/	/	1194872
	27	/	/	/	1068726
	28	/	/	/	925544
	29	/	/	/	755703
	30	/	/	/	534363

For sake of simplicity, the following nomenclature has been adopted (system = structure + dampers):

- system A-U: Type A structure equipped with U dampers;

10

- system B-U: Type B structure equipped with U dampers;

- system B-SP: Type B structure equipped with SP dampers.

Clearly, for the Type A structure, the SP and U damper distributions are coincident.

3.2. The seismic input and the dynamic analyses

An ensemble of 50 recorded ground motions (Hatzigeorgiou and Beskos 2009, Palermo et al. 2013b) has been used to perform the time-history analyses. The accelerograms have been selected from the PEER strong motion database in order to be representative of ground motions recorded in a type B soil according to the Italian building code (NTC 2008) and scaled to the same peak ground acceleration (PGA = 1.0g).

The average pseudo-acceleration S_a spectra (corresponding to 5% and 30% damping ratios) are displayed in Figure 2, while Figure 3 displays the ratio of the average velocity (V) / pseudo-velocity (S_v) spectrum (corresponding to 5% and 30% damping ratios).

Time-history analyses have been developed:

- either by direct integration of the equations of motion using the unconditionally stable Newmark method (Hilber et al. 1977). These analyses will be hereafter referred to as Response History Analyses, RHA (Chopra, 1995);

- or by integration based upon the response of the first mode of vibration only. These analyses will be hereafter referred to as 1st Modal Response Analysis, 1-MRA (Chopra, 1995).

The combined use of both RHA and 1-MRA allows to compare the inter-storey velocities due to all modes with the inter-storey velocities due to the first mode only, and thus to quantify the higher modes contribution.
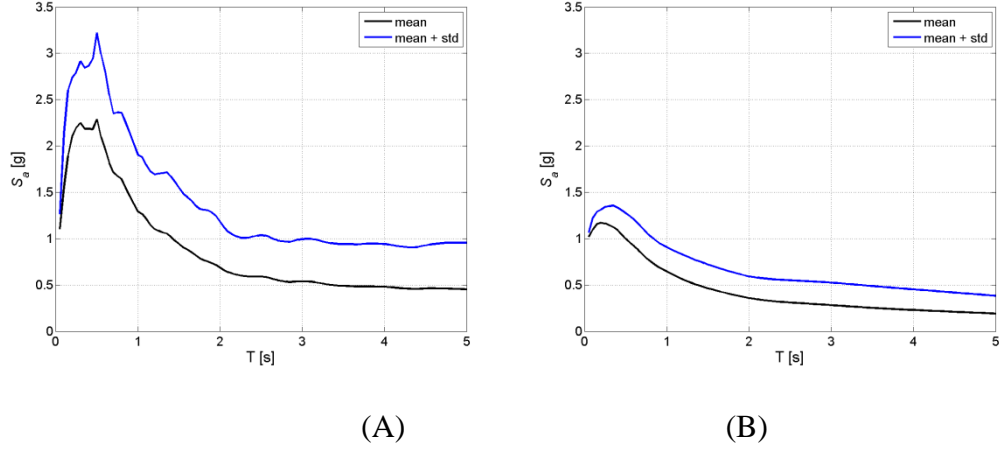
(A)   (B)

Figure 2 Mean and mean plus on standard deviation pseudo-acceleration spectra:
(A) ξ=0.05; (B) ξ=0.30.
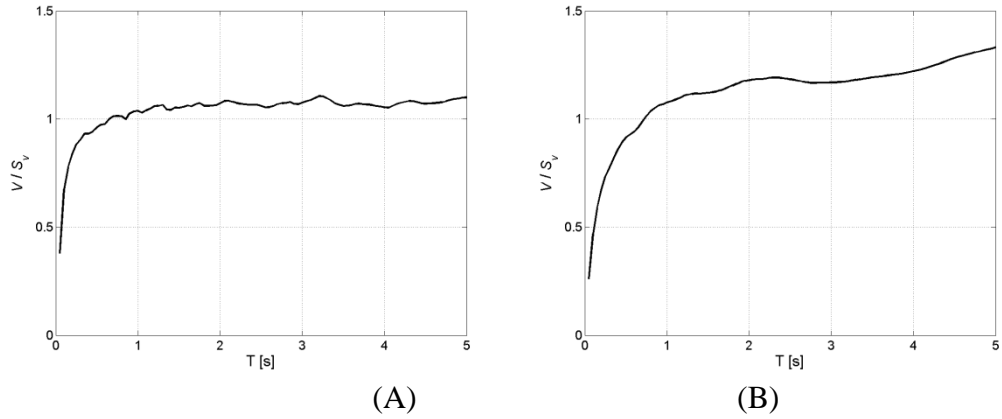

(A)   (B)

Figure 3 Mean Velocity/Pseudo-velocity spectra: (A) ξ=0.05; (B) ξ=0.30.
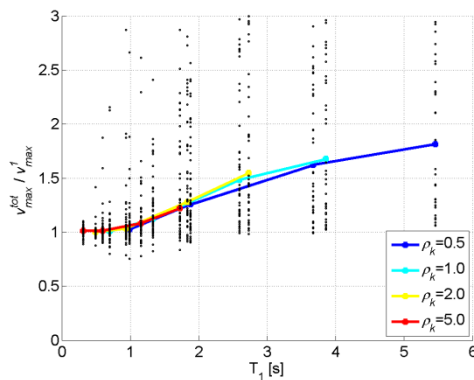
3.3. Main results

In this section, the following response quantities are illustrated and discussed:

- the maximum total first inter-storey velocity (as obtained from RHA), referred to as v_{max}^{tot};

- the maximum first inter-storey velocity due to the first mode only (as obtained from 1-MRA), referred to as v_{max}^{1};

- the maximum value of the peak inter-storey pseudo-velocity vector, as given by the predictive formulas derived in section 2 (Eq. (10): $v_{max,A}$ and Eq. (12): $v_{max,B}$).
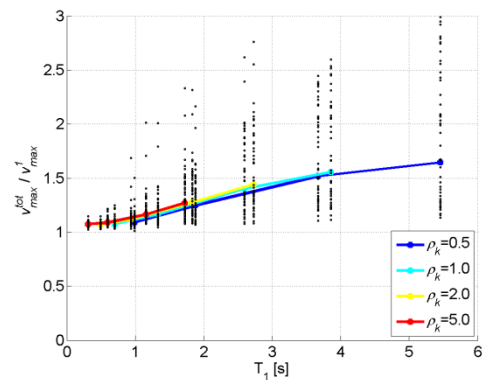
Figure 4 provides the ratios of $v_{max}^{tot}/v_{max}^{1}$ as a function of the fundamental period of the structure, T_1. Inspection of these plots allows the following fundamental observations:

12

- all three systems (A-U, B-U and B-SP) show similar trends of behaviour: the ratio v_{max}^{tot}/v_{max}^1 tends to increase (almost linearly) as the fundamental period and/or the total number of storeys increases. This effect is due to an increase in the higher modes contribution as clearly explained in a recent work by some of the authors (Palermo et al., 2015) which introduced the concept of Seismic Modal Contribution Factor as an improvement of the well-known Modal Contribution Factor (Chopra, 1995).

- on average, the maximum values of the ratio v_{max}^{tot}/v_{max}^1 are around 2.0.

- for short fundamental periods (say less than 1 s), the ratio v_{max}^{tot}/v_{max}^1 is lower than 1.0.

- the damping ratio seems to not significantly affect the ratio v_{max}^{tot}/v_{max}^1.

- the dispersion of the results is quite large.
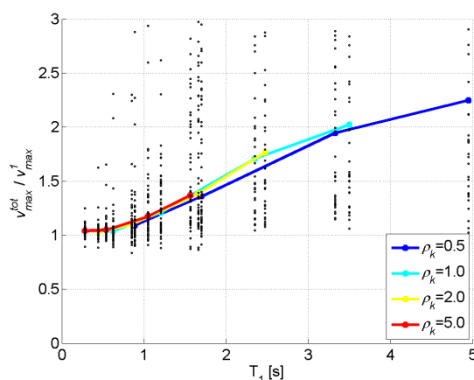
The results in terms of v_{max}^{tot}/v_{max}^1 ratios are similar to those obtained by Miranda and Akkar (2006) which noted that for large periods the inter-storey drift demand is significantly influenced by the higher modes. Nonetheless, the authors did not provide a formula for the prediction of this influence.
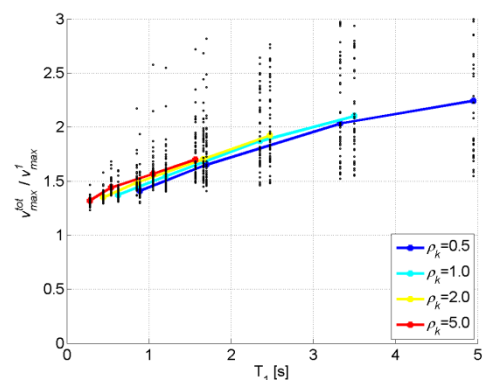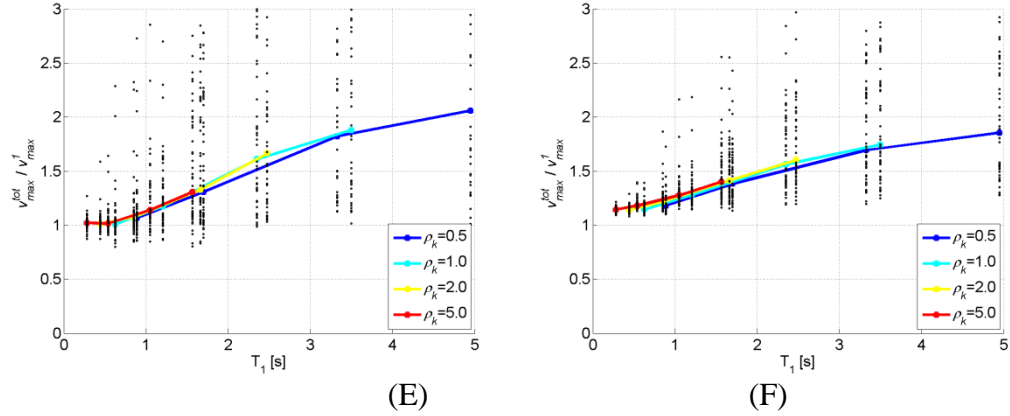

(A)

(B)

(C)

(D)

(E)   (F)

Figure 4 v_{max}^{tot}/v_{max}^1 vs T_1: (A) System A-U, ξ=0.05; (B) System A-U, ξ=0.30; (C) System B-U, ξ=0.05; (D) System B-U, ξ=0.30; (E) System B-P, ξ=0.05; (E) System B-P, ξ=0.30.

Figure 5 provides the ratios of $v_{max}^1/v_{max,A}$ and $v_{max}^1/v_{max,B}$ as a function of the fundamental period of the structure, T_1. Inspection of these plots allows the following fundamental observations:

- all three systems (A-U, B-U and B-SP) show similar trends of behaviour: on average, the ratios $v_{max}^1/v_{max,A}$ and $v_{max}^1/v_{max,B}$ are close to one for all systems.

- for short periods (say smaller than 0.5 s) and especially for $\xi = 0.30$, the ratios $v_{max}^1/v_{max,A}$ and $v_{max}^1/v_{max,B}$ tend to become smaller than 1.0.

- for high periods (say larger than 1.0 s) and independently from the damping ratio ξ, the ratios $v_{max}^1/v_{max,A}$ and $v_{max}^1/v_{max,B}$ are slightly larger than 1 (between 1.0 and 1.2).

- the dispersion of the results is quite large.

Note that the trends of the ratios $v_{max}^1/v_{max,A}$ and $v_{max}^1/v_{max,B}$ are in line with the trends of the average velocity/pseudo-velocity spectra represented in Figure 3 as also well described in the work by Peckan et al. (1999) which clearly identify the differences between the actual velocity and pseudo-velocity spectra.
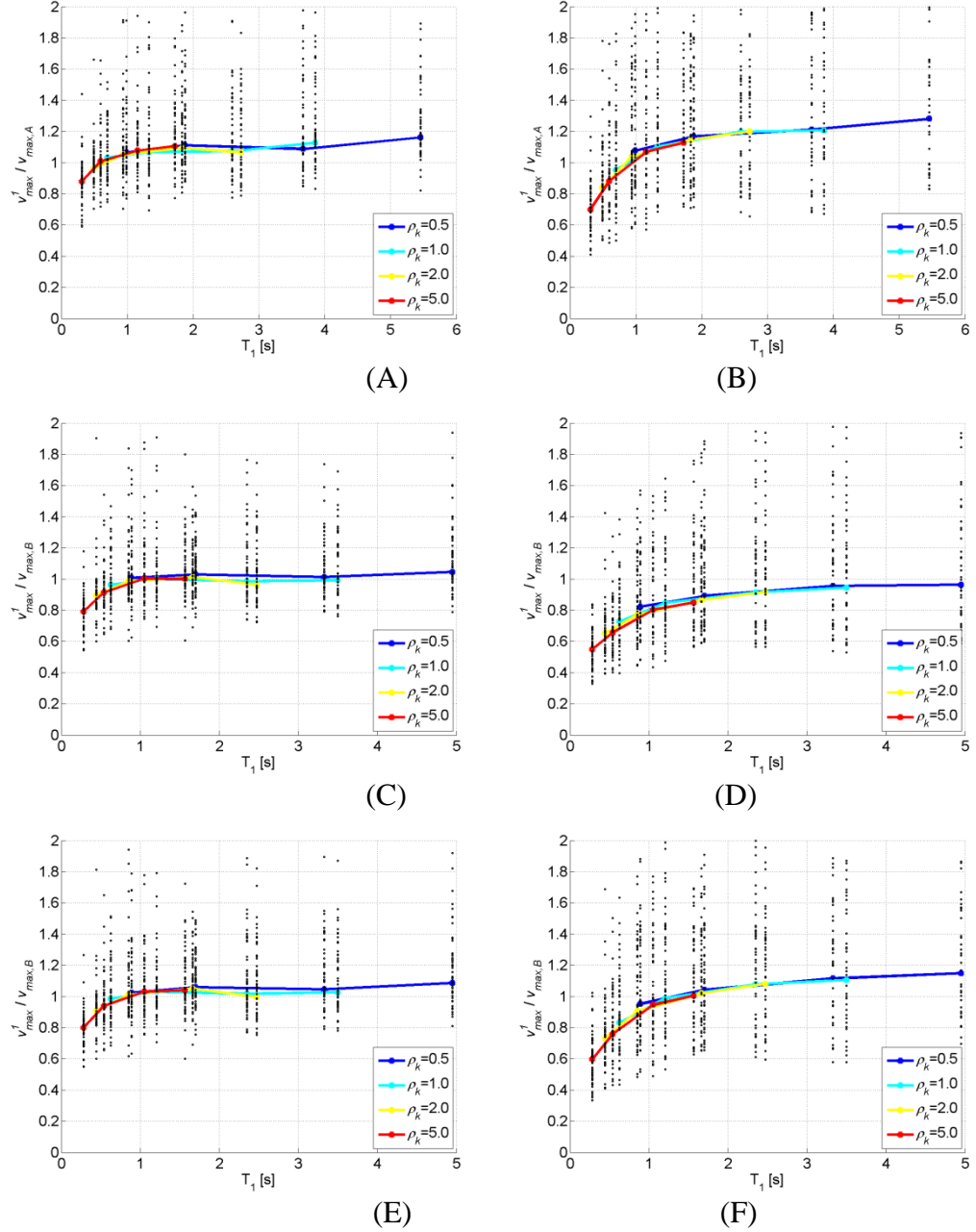
Figure 5 $v^1_{max} / v_{max,A}$ vs T_1: (A) System A-U, ξ=0.05; (B) System A-U, ξ=0.30. $v^1_{max} / v_{max,B}$ vs T_1: (C) System B-U, ξ=0.05; (D) System B-U, ξ=0.30; (E) System B-P, ξ=0.05; (F) System B-P, ξ=0.30.

3.4. A prediction for the maximum inter-storey velocities

Based on the results of the numerical simulations discussed in the previous section (3.3), a correction factor M can be introduced to account for the higher modes contribution, leading to the following estimation of the peak inter-storey velocities:

$$v_{\text{max},A,corrected} = \frac{v_{\text{max}}^{tot}}{v_{\text{max}}^{1}} \cdot v_{\text{max},A} = M \cdot v_{\text{max},A} \tag{14}$$

$$v_{\text{max},B,corrected} = \frac{v_{\text{max}}^{tot}}{v_{\text{max}}^{1}} \cdot v_{\text{max},B} = M \cdot v_{\text{max},B} \tag{15}$$

where M is a magnification factor obtained starting from linear regression analysis (Least Square Fit) of the results obtained from numerical simulations:

$$M = \frac{v_{\text{max}}^{tot}}{v_{\text{max}}^{1}} \cong \begin{cases} 1.0 & \text{for} \quad T \leq 0.5s \\ 0.31 \cdot T + 0.85 & \text{for} \quad 0.5 < T \leq 5.0s \end{cases} \tag{16}$$

Figure 6 compares the expression of M as given by Eq. (16) with the six regression lines as obtained for all the analyzed systems. Note that the six regression lines are close to each other and that, for safety reasons, Eq. (16) has been calibrated to be roughly larger than all six actual regression lines. The proposed equation of M, i.e. Eq. (16), appear suitable for both uniform (or nearly uniform) shear-type buildings or for more regular general moment resisting frame buildings where the first mode drift profile is linear (or nearly linear).
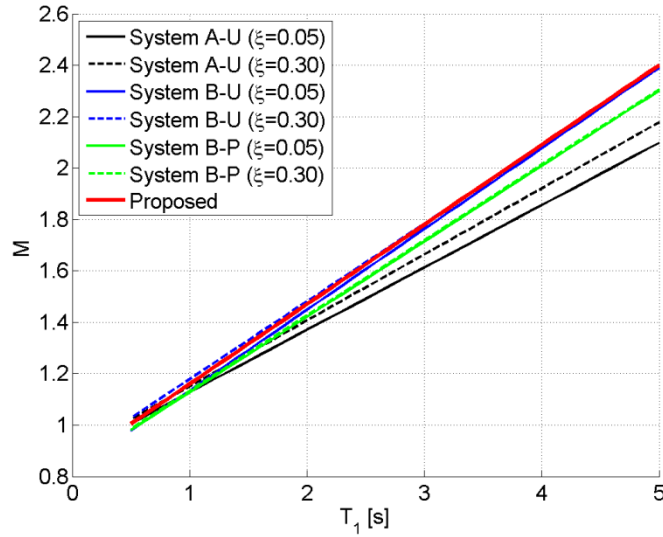

Figure 6 Magnification factor M as a function of the fundamental period T_1.

4. THE DIRECT FIVE-STEP PROCEDURE FOR THE DIMENSIONING OF ADDED VISCOUS DAMPERS

In 2010, some of the authors proposed the so-called five-step procedure for the design of frame structures equipped with added viscous dampers. The steps of the original procedure can be summarized as follows:

STEP 1: identification of the target damping ratio $\bar{\xi}$ leading to a certain target performance $\bar{\eta}$ (e.g. base shear, maximum inter-storey drift, …);

STEP 2: identification of the linear damping coefficients c_L for preliminary design purposes, by using the following formula:

$$c_L = \bar{\xi} \cdot \omega_1 \cdot m_{tot} \cdot \left(\frac{N+1}{n} \right) \cdot \frac{1}{\cos^2 \theta} \qquad (17)$$

where n is the total number of equally sized viscous dampers placed at each storey in a given direction and θ is the inclination of the dampers with respect to the horizontal direction.

STEP 3: development of linear numerical time-history analyses of the building structure equipped with the linear viscous dampers identified in Step 2. The aim is to identify the range of "working" velocities, $v_{\max}$, for the linear dampers.

STEP 4: identification of the target characteristics of the actual non-linear viscous dampers (damping coefficient $c_{NL} = \overline{c_{NL}}$, exponent $\alpha = \bar{\alpha}$, and axial stiffness of the device $k_{axial} = \bar{k}_{axial}$), i.e. identification of a system of manufactured viscous dampers capable of providing the structure with similar performances to those obtained in Step 3 with the linear viscous dampers sized in Step 2, by using the following formulas:

$$c_{NL} = c_L \cdot \left(0.8 \cdot v_{\max} \right)^{1-\bar{\alpha}} \qquad (18)$$

$$k_{axial} \geq 10 \cdot c_L \cdot \omega_1 \qquad (19)$$

STEP 5: verification of the performances of the structure equipped with the non-linear viscous dampers sized in Step 4 through non-linear numerical time-history analyses.

For more details and for all the notations which will be used hereafter, the interested reader is referred to the work by Silvestri et al. 2010.

It is worth noticing that, in the light of the results presented in the previous sections, the original procedure can be updated by substituting the numerical time-history analyses of Step 3 with the analytical predictive formulas for the maximum velocities, as given by Eq. (14) and (15). This leads to the following formulas for the non-linear damping coefficients (Step 4):

$$c_{NL,A} = c_L \cdot \left(0.8 \cdot v_{max,A} \cdot \cos\theta\right)^{1-\bar{\alpha}} = \bar{\xi} \cdot \omega_1 \cdot m_{tot} \cdot \left(\frac{N+1}{n}\right) \cdot \frac{1}{\cos^2\theta} \cdot \left(M \cdot 0.8 \cdot \frac{S_a}{\omega_1} \cdot \frac{12N}{(2+5N+5N^2)} \cdot \cos\theta\right)^{1-\bar{\alpha}}$$

(20)

$$c_{NL,B} = c_L \cdot \left(0.8 \cdot v_{max,B} \cdot \cos\theta\right)^{1-\bar{\alpha}} = \bar{\xi} \cdot \omega_1 \cdot m_{tot} \cdot \left(\frac{N+1}{n}\right) \cdot \frac{1}{\cos^2\theta} \cdot \left(M \cdot 0.8 \cdot \frac{S_a}{\omega_1} \cdot \frac{2}{N+1} \cdot \cos\theta\right)^{1-\bar{\alpha}}$$

(21)

If c_L is assumed equal for all dampers at all storeys and recalling that the estimate of $v_{max,B}$ holds for all stories, $c_{NL,B}$ is equal for all dampers at all storeys, i.e. the same manufactured dampers can be placed at all storeys. On the contrary, recalling that the estimate of $v_{max,A}$ holds only for the first storey, Eq. (20) may be rigorously applied only for the first storey. However, if the $c_{NL,A}$ value provided by Eq. (20) is used at all storeys, conservative design is achieved.

In addition, the preliminary design (Steps 1 to 4) of viscous dampers can be fully developed by means of analytical formulae, which can be also summarized in a single direct formula for the maximum damper force of non-linear viscous dampers:

$$F_{NL,A} = c_{NL,A} \cdot v_{max,A}^{\bar{\alpha}} = 0.8^{1-\bar{\alpha}} \cdot \bar{\xi} \cdot m_{tot} \cdot \frac{1}{n \cdot \cos\theta} \cdot M \cdot S_a\left(T_1, \bar{\xi}\right) \cdot \frac{12N(N+1)}{(2+5N+5N^2)}$$

(22)

$$F_{NL,B} = c_{NL,B} \cdot v_{max,B}^{\bar{\alpha}} = 2 \cdot 0.8^{1-\bar{\alpha}} \cdot \bar{\xi} \cdot m_{tot} \cdot \frac{1}{n \cdot \cos\theta} \cdot M \cdot S_a\left(T_1, \bar{\xi}\right)$$

(23)

It is clear that the final design verification (Step 5) still should be carried out by means of non-linear numerical time-history analyses.

18

5. APPLICATIVE EXAMPLE

5.1. The case study and the retrofitting strategy

A R/C school building in Italy is analyzed in this section. The 3-storey building, situated in Bisignano (Cosenza, southern Italy), was assumed as a benchmark structure for a Research Project financed by the Italian Department of Civil Protection, with the aim of studying its seismic behaviour, as well as of proposing and comparing alternative retrofitting solutions based on different seismic protection strategies. A detailed description of the building is available in the works by Sorace and Terenzi (2014) and Mazza and Vulcano (2014). The former analyzed the effectiveness of two retrofitting solutions based on (1) a dissipative bracing system incorporating pressurized fluid viscous spring-dampers; and (2) a base isolation system including double friction pendulum sliding bearings. The latter studied a retrofitting solution based on the use of chevron steel braces equipped with hysteretic dampers (HYDs).
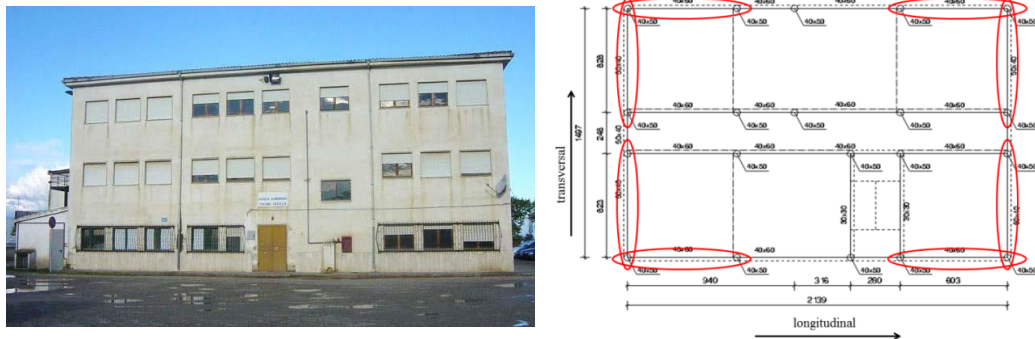

Figure 7 Front view and plan view of the case study building with indication of the bays in which the dampers are placed

The numerical simulations have been developed using the software SAP 2000 NL v16. A group of seven artificial records have been generated by SIMQKE (Vanmarke et al. 1990) in order to match the design spectrum according to the Italian building code NTC08.
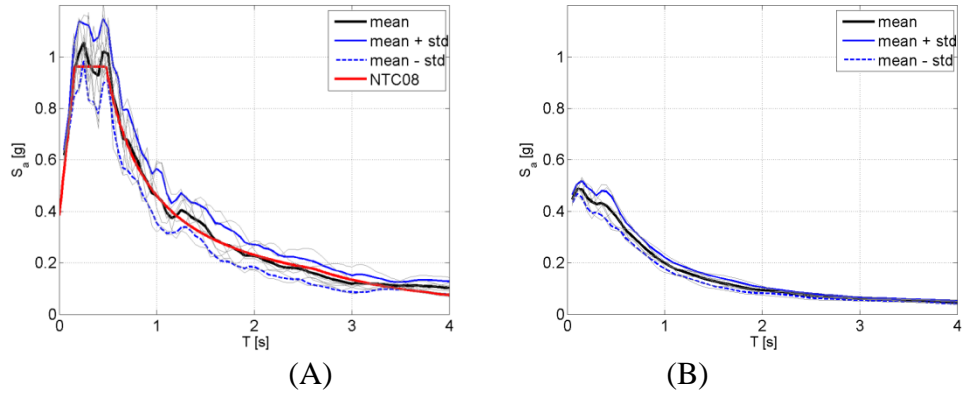
Figure 8 Response spectra of the 7 artificial records: (A) 5% damping ratio; (B) 30% damping ratio.

The seismic weight of the building W_{tot} is approximately equal to 11900 kN, while the first three periods (two mainly translational and one mainly rotational) of the naked frame structure (without the non-structural masonry infills) are equal to 0.80s (mainly translational along the y-direction), 0.52s (mainly rotational) and 0.45s (mainly translational along the x-direction), respectively. The significant difference in the first two translational periods is due to the absence of primary beams (excluding the secondary perimeter beams) along the y-direction. This leads to a nearly linear first-mode shape along the y-direction, as shown in Fig. 9B. Thus, profile B has been selected for the y-direction. As highlighted in section 4, by assuming the same c_L for all dampers, the formulation based on profile B leads to equal dampers at all stories. Given that, in practical applications, for economic purposes, it is convenient, and thus common, to adopt equal dampers, the formulation based on profile B (which leads to equal dampers at all stories) has been also applied to the x-direction.

The retrofitting strategy here adopted is based on the insertion of inter-storey viscous dampers. In detail, four inter-storey viscous dampers are supposed to be located at each floor along both the longitudinal and the transversal directions, as shown in the plan view of the building (Figure 7). The damper system is therefore composed of 24 viscous dampers and is designed according to the direct five-step procedure introduced in previous sections. For the final verification of the effectiveness of the designed damper system (i.e. Step 5 of the procedure), three numerical models have been developed:

- the naked structure, i.e. the building structure without added dampers (UND model);

- the building structure equipped with linear viscous dampers (D-L model);
- the building structure equipped with non-linear viscous dampers (D-NL model).

A 3D view of the FE model of the building equipped with the added viscous dampers is given in Figure 9.

(A)

(B)

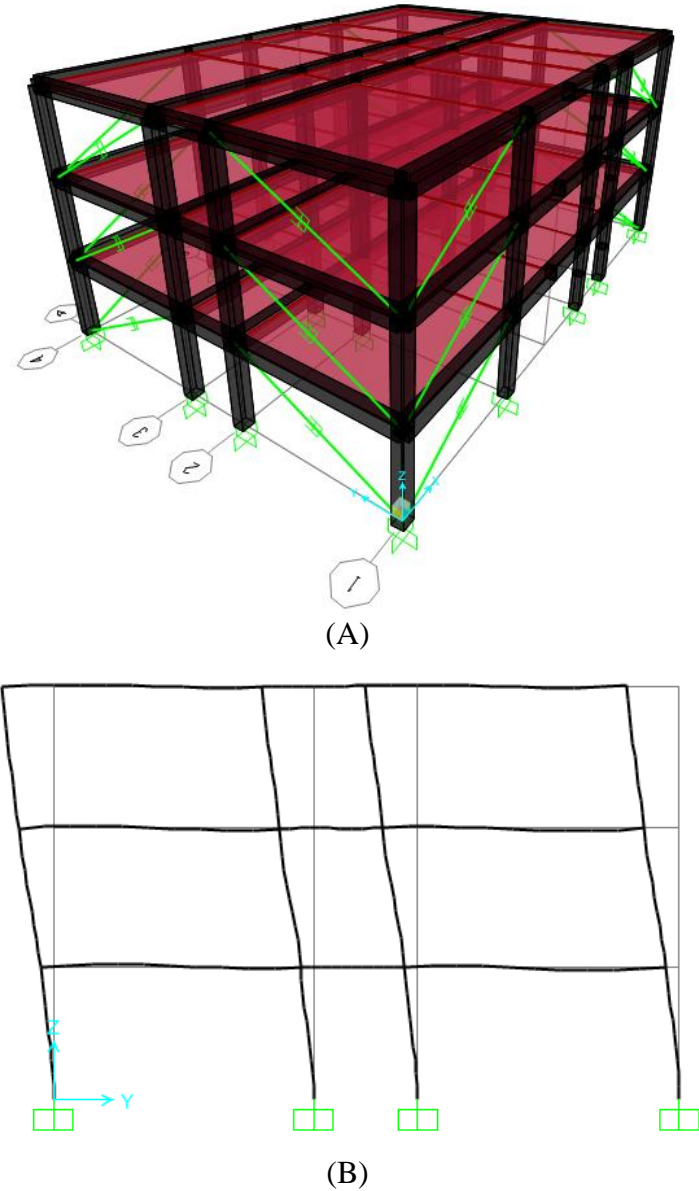Figure 9. (A) SAP 2000 model of the structure equipped with inter-storey viscous dampers. (B) first-mode deformed shape (planar view) along the y-direction.

5.2. The design of the added viscous dampers according to the direct five-step procedure (steps 1-4)

A target damping ratio $\bar{\xi} = 0.30$ has been chosen in order to design the system of added viscous dampers. The added dampers are designed according to the direct

five-step procedure assuming a linear deformed shape and equal dampers at all storeys (i.e. formulation based on profile B). The main properties of the added linear and non-linear dampers are summarized in Table 1. A damper exponent α=0.15 has been chosen for the non-linear dampers (FIP 2013).

Table 1: Properties of the nonlinear dampers.

	c_L (Eq. 17) [kN s/m]	α	v_{max} (Eq. 15) [m/s]	$c_{NL,B}$ (Eq. 21) [kN s$^{0.15}$/m$^{0.15}$]
Along x	5332	0.15	0.14	831
Along y	3000	0.15	0.15	511

5.3. Step 5: Final verification through non-linear time history analyses

Figure 10 displays the average (over the seven accelerograms) peak inter-storey velocities profiles as obtained from the numerical simulations with the ones predicted according to Eq. (15). The trends along the two directions exhibit some differences. On average, the prediction along the y-direction fit well with the average profile as obtained from the linear analyses, while the prediction along the x-direction is more conservative. The average peak velocity profiles obtained from the non-linear simulations is a consequence of this result: along the x-direction the peak velocities are further reduced with respect to linear response (meaning that along the x-direction the non-linear dampers are more effective than the linear ones).

The averages (over the seven accelerograms) of the maximum values of the base shear, as obtained for the UND, the D-L and the D-NL models are reported in Table 2. Also, the damping reduction factor of the base shear ($\eta = \dfrac{V_{base,D}}{V_{base,UND}}$) is reported. Note that, for a target damping ratio of $\overline{\xi} = 0.30$, the widely used formulation by Bommer et al. (2000) leads to $\overline{\eta} = 0.53$. It is to be noted that both linear models lead to damping reduction factors of the base shear smaller (and thus more conservative) than the target one ($\overline{\eta} = 0.53$). When looking to the response of the non-linear models, the conservativeness along the x-direction even increases as above observed (see Figure 10). From a design point of view, the amount of reduction in the base shear is similar to that obtained by employing the

two alternative solutions proposed in the work by Sorace and Terenzi (2014), namely: (1) the use of dissipative bracings, and (2) the introduction of a base isolation system including double friction pendulum sliding bearings.

Table 3 compares the averages (over the seven accelerograms) of the maximum values of the damper forces in the non-linear dampers at each floor with the predicted ones using Eq. (23). Note that, from an engineering point of view, excluding the top storey along the x direction, the average relative errors in the estimation of the damper forces are reasonable.

The larger discrepancies between the numerical results and the analytical predictions along the x-direction are probably related to the simplified assumption of equal dampers at all stories, since along the x-direction the assumption of linear first mode shape could be less appropriate than along the y-direction.

It should be acknowledged that similar results in terms of accuracy of predictions were obtained by Ramirez et al. (2003) for 3-storey yielding structures with linear and non-linear dampers.
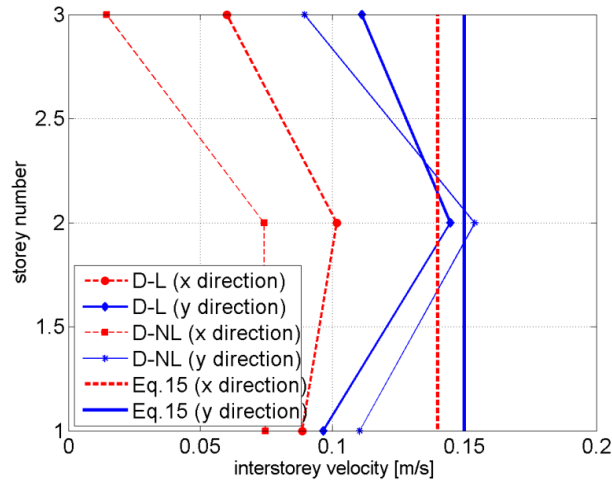
Figure 10. Peak inter-storey velocity profiles.

Table 2: Reduction in the base shear.

		UND	D-L	D-NL
along X direction	V_{base} [kN]	9777	3840	2646
	η		0.39	0.27
along Y direction	V_{base} [kN]	5258	2298	2416
	η		0.43	0.46

Table 3: Maximum damper forces in the non-linear dampers (x-direction).

	"actual" force (from numerical simulations) [kN]	prediction (Eq. (23)) [kN]	Relative difference [%] between the "actual" force and Eq. (23)
1st floor	560	620	10%
2nd floor	560	620	10%
3rd floor	440	620	29%

Table 4: Maximum damper forces in the non linear dampers (y-direction).

	"actual" force (from numerical simulations) [kN]	prediction (Eq. (23)) [kN]	Relative difference [%] between the "actual" force and Eq. (23)
1st floor	367	390	5%
2nd floor	385	390	1%
3rd floor	355	390	9%

6. CONCLUSIONS

In this paper, analytical estimations of the peak inter-storey velocities for framed building structures have been derived. The effectiveness of the formula in estimating actual peak inter-storey velocities has been investigated by means of extensive numerical simulations on shear-type frame structures with uniform and non-uniform storey stiffness. It has been shown that the analytical expressions are, on average, slightly conservative for low-medium rise frame structures (fundamental periods smaller than 1.0 s). For larger periods, a corrective coefficient (depending on the higher mode contribution), linearly increasing with the fundamental period, needs to be introduced. For tall buildings (say natural period around 3.0 s) the magnifications are around 2.5. The formulae are suitable when dealing with uniform or regular multistory frame buildings typically characterized by a nearly linear first mode shape. For more complex frame buildings (i.e. plan or in-elevation irregular structures) more appropriate analyses have to be developed.

The formulae have been then used to simplify the original procedure for the seismic design of building structures equipped with viscous dampers proposed by Silvestri *et al.* (2010), which requires the development of numerical simulations for the estimation of the damper working velocities, and thus to obtain a direct procedure.

The direct five-step procedure has been applied to a real case study, namely a RC school building located in southern Italy, assumed as a benchmark structure for a Research Project financed by the Italian Department of Civil Protection. It is found that the direct procedure, beside allowing an easy identification of the mechanical characteristics of the viscous dampers, leads to a conservative achievement of the target performances. Improved estimates of the main quantities can be obtained in the verification time-history analyses of Step 5.

Finally, it is worth to remark that the direct procedure is targeted to practitioners with no experience with the design of added viscous dampers. For more accurate results, as in the case of final design, other procedures (such as the original five-step procedure or the ASCE 7 (2005) Chapter 18 provisions), or even more complex procedures (based on algorithms and optimization methods) can be used.

ACKNOWLEDGEMENTS

REFERENCES

Adachi F, Fujita K, Tsuji M, Takewaki I (2013) Importance of interstory velocity on optimal along-height allocation of viscous oil dampers in super high-rise buildings. Engineering Structures, 56: 489-500.

Akkar S, Yazgan U, Gülkan P. (2005). Drift estimates in frame buildings subjected to near-fault ground motions. Journal of Structural Engineering, 131(7): 1014-1024.

American Society of Civil Engineers, ASCE 7–05 (2005) Minimum design loads for buildings and other structures. Reston, VA.

ASCE. (2005). Minimum design loads for buildings and other structures. ASCE/SEI 7-05 including Supplement No.1, Reston, VA.

Bommer JJ, Elnashai AS, Weir AG (2000) Compatible acceleration and displacement spectra for seismic design codes. In: Proceedings of the 12th World Conference on Earthquake Engineering. Auckland, New Zealand.

Chopra AK (1995) Dynamics of structures. Theory and applications to earthquake engineering. Prentice-Hall, Upper Saddle River.

Christopoulos C, Filiatrault A (2006) Principles of passive supplemental damping and seismic isolation. IUSS Press, Pavia.

Constantinou MC, Soong TT, Dargush GF (1998) Passive energy dissipation systems for structural design and retrofit, monograph No. 1. Multidisciplinary Center for Earthquake Engineering Research, Buffalo, New York.

Constantinou MC, Symans MD (1992) Experimental and analytical investigation of seismic response of structures with supplemental fluid viscous dampers. NCEER-92-0032. National Center for Earthquake Engineering Research, Technical report, Buffalo.

Constantinou MC, Symans MD (1993) Seismic response of structures with supplemental damping. Struct Des Tall Build 2:77–92.

Constantinou MC, Tadjbakhsh IG (1983) Optimum design of a first story damping system. Comput. Struct. 17(2):305–310.

Diotallevi PP, Landi L, Dellavalle A (2012) A methodology for the direct assessment of the damping ratio of structures equipped with nonlinear viscous dampers. J Earthq Eng 16:350–373.

Filiatrault A, Leger P, Tinawi R (1994) On the computation of seismic energy in inelastic structures. ASCE Journal of Structural Engineering, 116(5): 1334-1355.

FIP (2013). Anti-seismic devices product division. http://www.fip-group.it.

Hart GC, Wong K (2000) Structural dynamics for structural engineers. Wiley, New York.

Hatzigeorgiou GD, Beskos DE (2009) Inelastic displacement ratios for SDOF structures subjected to repeated earthquakes. Eng Struct 31:2744–2755.

Hilber HM, Hughes TJ, Taylor, L. (1977). Improved numerical dissipation for time integration algorithms in structural dynamics. Earthquake Engineering and Structural Dynamics, 5(3): 283-292.

Hwang JS, Lin WC, Wu NJ (2013) Comparison of distribution methods for viscous damping coefficients to buildings. Struct Infrastruct Eng 9(1):28–41.

Landi L, Diotallevi PP, Castellari G (2013) On the Design of Viscous Dampers for the Rehabilitation of Plan-Asymmetric Buildings. Journal of Earthquake Engineering 17(8):1141-1161.

Landi L, Lucchi S, Diotallevi PP (2014) A Procedure for the Direct Determination of the Required Supplemental Damping for the Seismic Retrofit with Viscous Dampers. Engineering Structures, 71: 137-149.

Levy R, Lavan O (2006) Fully stressed design of passive controllers in framed structures for seismic loadings. Struct Multidiscip Optimiz 32(6):485–498.

Lopez Garcia D (2001) A simplemethod for the design of optimal damper configurations in MDOF structures. Earthq Spectra 17(3):387–398.

Mazza F, Vulcano A (2014) Equivalent viscous damping for displacement-based seismic design of hysteretic damped braces for retrofitting framed buildings. Bulletin of Earthquake Engineering, 12(6): 2797-2819.

Miranda E, Akkar SD (2006). Generalized interstory drift spectrum. Journal of Structural Engineering, 132(6): 840-852.

NTC (2008) Norme Tecniche per le Costruzioni, Italian building code, adopted with D.M. 14/01/2008, published on S.O. n. 30 G.U. n. 29 04/02/2008.

Occhiuzzi A (2009) Additional viscous dampers for civil structures: analysis of design methods based on effective evaluation of modal damping ratios. Eng Struct 31(5):1093–1101.

Palermo M, Muscio S, Silvestri S, Landi L, Trombetti T (2013) On the dimensioning of viscous dampers for the mitigation of the earthquake-induced effects in moment-resisting frame structures. Bulletin of Earthquake Engineering, 11(6): 2429-2446.

Palermo M, Silvestri S, Gasparini G, Trombetti T (2015). Seismic Modal Contribution Factors. Bulletin of Earthquake Engineering, DOI 10.1007/s10518-015-9757-7.

Palermo M, Silvestri S, Trombetti T, Landi, L (2013). Force reduction factor for building structures equipped with added viscous dampers. Bulletin of Earthquake Engineering, 11(5): 1661-1681.

Pekcan G, Mander JB, Chen S (1999). Fundamental considerations for the design of non-linear viscous dampers. Earthquake Engineering and Structural Dynamics; 28: 1405-1425.

Ramirez OM, Constantinou MC, Kircher CA, Whittaker AS, Johnson MW, Gomez JD, Chrysostomou CZ (2000) Development and evaluation of simplified procedures for analysis and design of buildings with passive energy dissipation systems. MCEER-00-0010. Technical report, Buffalo.

Ramirez OM, Constantinou MC., Whittaker AS., Kircher CA, Chrysostomou CZ. (2002a). Elastic and inelastic seismic response of buildings with damping systems. Earthquake Spectra, 18(3), 531-547.

Ramirez OM., Constantinou MC, Gomez JD, Whittaker AS, Chrysostomou CZ. (2002b). Evaluation of simplified methods of analysis of yielding structures with damping systems. Earthquake Spectra, 18(3), 501-530.

Ramirez, OM, Constantinou MC, Whittaker AS, Kircher CA., Johnson MW, Chrysostomou CZ. (2003). Validation of the 2000 NEHRP provisions' equivalent lateral force and modal analysis procedures for buildings with damping systems. Earthquake Spectra, 19(4), 981-999.

Shukla, AK., and Datta, TK. (1999) Optimal use of viscoelastic dampers in building frames for seismic force. Journal of Structural Engineering ASCE 1999; 125 (4),: 401-409.

Silvestri S, Trombetti T (2007) Physical and numerical approaches for the optimal insertion of seismic viscous dampers in shear-type structures. J Earthq Eng 11(5):787–828.

Silvestri S, Gasparini G, Trombetti T (2010) A five-step procedure for the dimensioning of viscous dampers to be inserted in building structures. J Earthq Eng 14(3):417–447.

Silvestri S, Gasparini G, Trombetti T (2011). Seismic design of a precast r. c. structure equipped with viscous dampers. Earthquake and Structures, 2(3), 297-321.

Singh MP, Moreschi LM (2002) Optimal placement of dampers for passive response control. Earthq Eng Struct Dyn 31:955–976.

Soong TT, Dargush GF (1997) Passive energy dissipation systems in structural engineering.Wiley, Chichester.

Sorace S, Terenzi G (2014) Motion control-based seismic retrofit solutions for a R/C school building designed with earlier Technical Standards. Bulletin of Earthquake Engineering, 12:2723-2744.

Takewaki I (1997) Optimal damper placement for minimum transfer functions. Earthq Eng Struct Dyn 26:1113–1124.

Takewaki I (2000) Optimal damper placement for critical excitation. Prob Eng Mech 15:317–325.

Takewaki I (2009) Building control with passive dampers: optimal performance-based design for earthquakes. Wiley, Singapore.

Trombetti T, Silvestri S (2004) Added viscous dampers in shear-type structures: the effectiveness of mass proportional damping. J Earthq Eng 8(2):275–313.

Trombetti T, Silvestri S (2006) On the modal damping ratios of shear-type structures equipped with Rayleigh damping systems. J Sound Vib 292(2):21–58.

Trombetti T, Silvestri S (2007) Novel schemes for inserting seismic dampers in shear-type systems based upon the mass proportional component of the Rayleigh damping matrix. J Sound Vib 302(3):486–526.

Uang CM, Bertero VV (1990) Evaluation of seismic energy in Structures, Earthquake Engineering and Structural Dynamics, 19:77-90.

Vanmarcke EH, Cornell CA, Gasparini DA, Hou S (1990) SIMQKE-I: simulation of earthquake ground motions. T.F. Blake, Newbury Park, California, Department of Civil Engineering, Massachusetts Institute of Technology, Cambridge, Massachusetts, Modified.

Whittaker AS, Constantinou MC, Ramirez OM, Johnson MW, Chrysostomou CZ. (2003). Equivalent lateral force and modal analysis procedures of the 2000 NEHRP Provisions for buildings with damping systems. Earthquake Spectra, 19(4), 959-980.